Revista Brasileira de Física, Vol. 7, N? 2, 1977

Analysis of Distortion in Momentum Distributions Obtained from Quasí-Free (p, 2p) Processes

P. M. MORS, V. E. HERSCOVITZ* and GERHARD JACOB**
Instituto de Física, Universidade Federal do Rio Grande do Sul"", Porto Alegre RS*

Recebido em 20 de Dezembro de 1976

Results obtained from (p,2p) coplanar processes are presented as contour diagrams of momentum distributions. The influence of the complex optical potential on such diagrams is discussed. Explicit calculations have been performed for the reaction $^{16}O(p,2p)^{15}N$ at 200 and 380 MeV.

Resultados obtidos em processos (p,2p) coplanares são apresentados através de diagramas de contorno das distribuições de momentum. É discutida a influência do potencial óptico complexo sobre tais diagramas. Cálculos explícitos foram realizados para a reação $^{16}O(p,2p)^{15}N$, a 200 e 380 MeV.

1. INTRODUCTION

Quasi-free reactions give valuable information on nuclear structure[1,2], such as momentum distributions of individual nuclear hole states with complex[3] binding energies.

---

* Research Fellow, CNPq.

** Senior Research Fellow, CNPq.

***Postal address: Av. Luiz Englert, s/n, 90000-Porto Alegre RS.

The usual representation of such results is done in the form of energy spectra (cross section versus energy) and distorted momentum distributions (cross section versus momentum or angle.

It has been suggested[4] to present the information on (p,2p) distorted momentum distributions in the form of contour diagrams of these distributions; such a presentation could be helpful in obtaining information on the nuclear optical potential.

The purpose of this paper is to present some theoretical results on the properties of such diagrams. Calculations have been kept as simple as possible and have been performed for ^{16}O with proton incident energies of 200 and 380 MeV.

In Section 2, the method of calculation and the results are presented, and in Section 3 these results are discussed and some conclusions are drawn.

2. CONTOUR DIAGRAMS OF DISTORTED MOMENTUM DISTRIBUTIONS

This Section starts with a short outline of suggestions and arguments from Ref. 4 on contour diagrams.

Consider a coplanar (p,2p) reaction in which a medium-energy proton (150-1000 MeV) knocks out a nuclear proton. The residual nucleus having a recoil momentum $\vec{k}$, the distorted momentum distribution will be given in the Distorted Wave Impulse Approximation (DWIA) by

$$|g'|^2 \equiv |g'(\vec{k})|^2 = (2J_A + 1)^{-1} \sum \left| \int \exp(i\vec{k}.\vec{r}) \prod_{j=0}^{2} D_j(\vec{r}) \psi_{J_A M_A}(\vec{r}) d^3r \right|^2 , \quad (1)$$

where $\psi_{J_A M_A}(\vec{r})$ is the overlap integral between the initial and final states (a nuclear hole wavefunction), and the sum extends over all states within one energy peak. Using the WKB approximation, in order to take distortion by the optical potentials $V_j(\vec{r}) = U_j(\vec{r}) + iW_j(\vec{r})$ in-

to account, the distorting functions $D_j(\vec{r})$ for the incident $(j=0)$ and the two outgoing $(j=1,2)$ protons are given by

$$D_j(\vec{r}) = \exp\{-i(E_j/\hbar^2c^2k_j)\int V_j(\vec{r}+s\,\hat{k}_j)ds\}, \qquad (2)$$

the integrations being taken along the classical paths.

In the absence of distortion, $D_j(\vec{r}) = 1 (j=0,1,2)$ and $|g'|^2$ would depend only on $|\vec{k}|$, i.e., would be rotationally symmetric in $\vec{k}$-space. In general, $|g'|^2$ is not rotationally simmetric because $\prod_{j=0}^{2} D_j$ introduces additional momentum components which are asymmetric and depend strongly on the geometry.

For the energies which are considered, the recoil momentum $\vec{k}$ is in general much smaller than the momenta of the incident and outgoing protons; thus, starting from a certain geometry, it is possible to scan the momentum distributions changing the geometry only slightly. In such a situation, the D_j's, and consequently the product $\prod_{j=0}^{2} D_j(\vec{r})$, in Eq. (1), are approximately independent of the direction of the recoil momentum. As seen from Eqs. (1) and (2), the real parts of the V_j's will introduce phase factors of the form $\exp(i\vec{a}_j.\vec{r})$, $\vec{a}_j$ being related to $U_j(\vec{r})$, and the imaginary parts will introduce factors of the type $\exp(-\vec{b}_j.\vec{r})$, $\vec{b}_j$ being related to $W_j(\vec{r})$.

Consider now the diagrams of constant values of the momentum distributions in the plane of the recoil momentum components (contour diagrams in $\vec{k}$-space). The idealized situation of undistorted momentum distributions ($|g'|^2$ rotationally symmetric) would lead to circles around the origin for these contour diagrams. In the actual situation, due to the effect of the optical potentials, the contour diagrams will not be rotationally symmetric anymore.

As compared to the idealized undistorted plots, the actual contour diagrams will show a shift in the origin, due to the effective momenta [5] of the incident and outgoing particles inside the nucleus (caused by the real parts of the optical potentials), and a change in magnitude, due mainly to the absorption of the protons by the residual nucleus

(caused by the imaginary parts of the optical potentials). Both effects are, of course, energy dependent and the analysis of contour diagrams could help in better visualizing the influence of the optical potentials. Gustafsson and Berggren[6] have studied the effect of the distortion on contour diagrams in configuration space.

To show these effects, calculations have been performed for the reaction $^{16}O(p,2p)^{15}N$, as mentioned in Section 1. The overlap integral $\psi_{J_A M_A}(\vec{r})$ has been taken as a single particle wavefunction generated by an infinite harmonic oscillator potential (without spin-orbit coupling) and the distorting potentials have been taken as square wells.

The geometry, given in Fig. 1, is coplanar, approximately symmetric, the momentum of the incident proton being parallel to the k_x direction; deviations from the symmetric situation have been achieved by varying the angles ϕ_1 and ϕ_2, the energies of the outgoing protons being kept equal. Care has been taken that, in general, not too strong deviations from the symmetric situation occur.

The wavefunctions for ^{16}O have been taken as harmonic oscillator ones, with the parameter $\gamma = \left(\frac{m\omega}{\hbar}\right)^{1/2}$ fixed so as to fit the radius obtained by electron scattering: $\gamma = 0.568$ fm^{-1}. The separation energies S_1 and S_0 of the single proton states have been taken, as $S_1 = 16.3$ MeV (the weighted average of the two 1p energies) and $S_0 = 44.0$ MeV.

The radius of the square well opticai potential has been taken equal to the equivalent uniform radius of ^{16}O, $R = 3.41$ fm, and the form factors of the real and imaginary parts have been taken equal, so that for $r < R$

$$\frac{U_j(\vec{r})}{W_j(\vec{r})} = \alpha_j \ , \qquad (3)$$

α_j being independent of $\vec{r}$.

Thus, one obtains for Eq. (2) the sbmple form

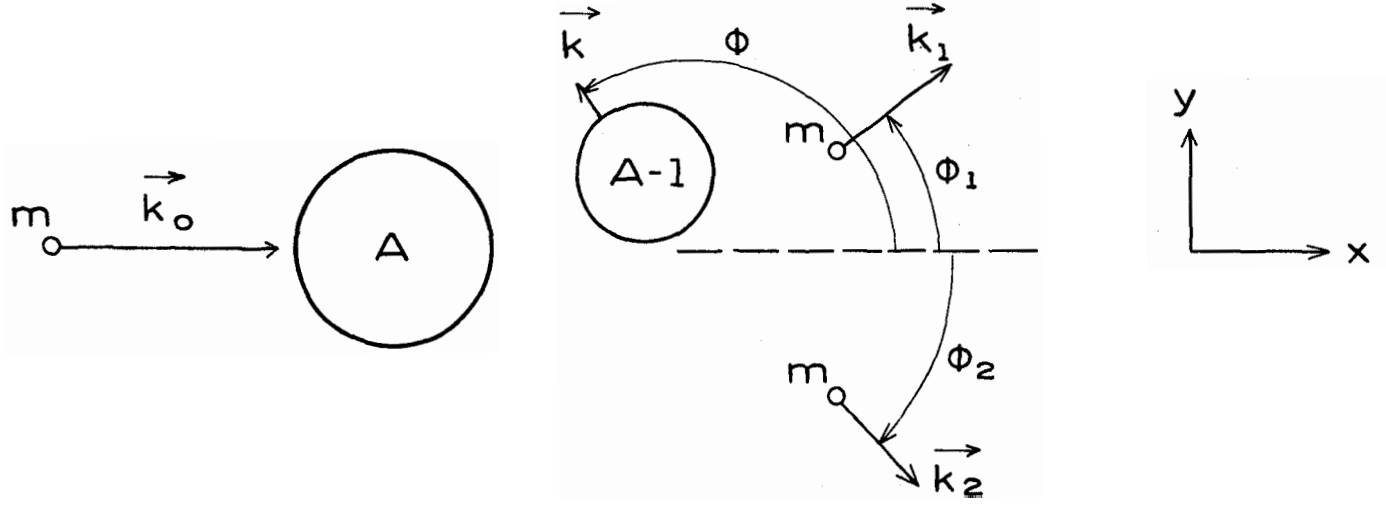

Fig. 1. The geometry of the **process.**

$$D_j(\vec{r}) = \exp\left[\frac{1}{2\lambda_j}(i\alpha_j - 1)\, d_j(\vec{r})\right], \quad j = 0,1,2, \qquad (4)$$

$d_j(\vec{r})$ being the classical paths of the protonç. The imaginary part of the optical potential is related to h_3 by $W_j(\vec{r}) = -\hbar^2 c^2 k_a / 2E_a \lambda_j$; in the case of the square well, h_3 is the mean free path of the proton in the nucleus.

The parameters of the optical potentials have been fixed between 180 and 380 MeV using the results of Ref. 7 for α_3 and W_j, and between 80 and 300 MeV using the results of Ref. 8 for U_3 and W_j, corrected for the difference in r_0 ($r_0 = R\, A^{-1/3}$) for ^{16}O and for nuclear matter by the ratio $(\frac{1.10}{1.35})^3$. The results of the two determinations agree well in the region where a comparison is possible. Table 1 shows the values of the parameters used in the calculation.

In Figs. 2 and 3, we present the results for the 1s and 1p states of ^{16}O respectively, at an incident energy of 380 MeV, considering only the real parts of the optical potentials (dashed lines), only the imaginary parts (thin full lines) and the complete complex potentials (thick full lines); the points are the calculated ones. The curves are symmetric around the k_x line, as expected from the behaviour of the integrand of Eq.(1) under the exchange $\phi \to 2\pi - \phi$. In Figs. 4 and 5, similar results for an incident energy of 200 MeV are presented.

Incident kinetic energy (MeV)	Nuclear state	a for the incoming proton	a for the outgoing protons	λ for the incoming proton (fm)	λ for the outgoing protons (fm)
380	1s	0.25	1.03	4.49	4.05
	1p	0.25	0.94	4.49	4.15
200	1s	0.80	2.34	4.26	3.26
	1p	0.80	2.04	4.26	3.69

Table 1. Parameters used in the calculation.

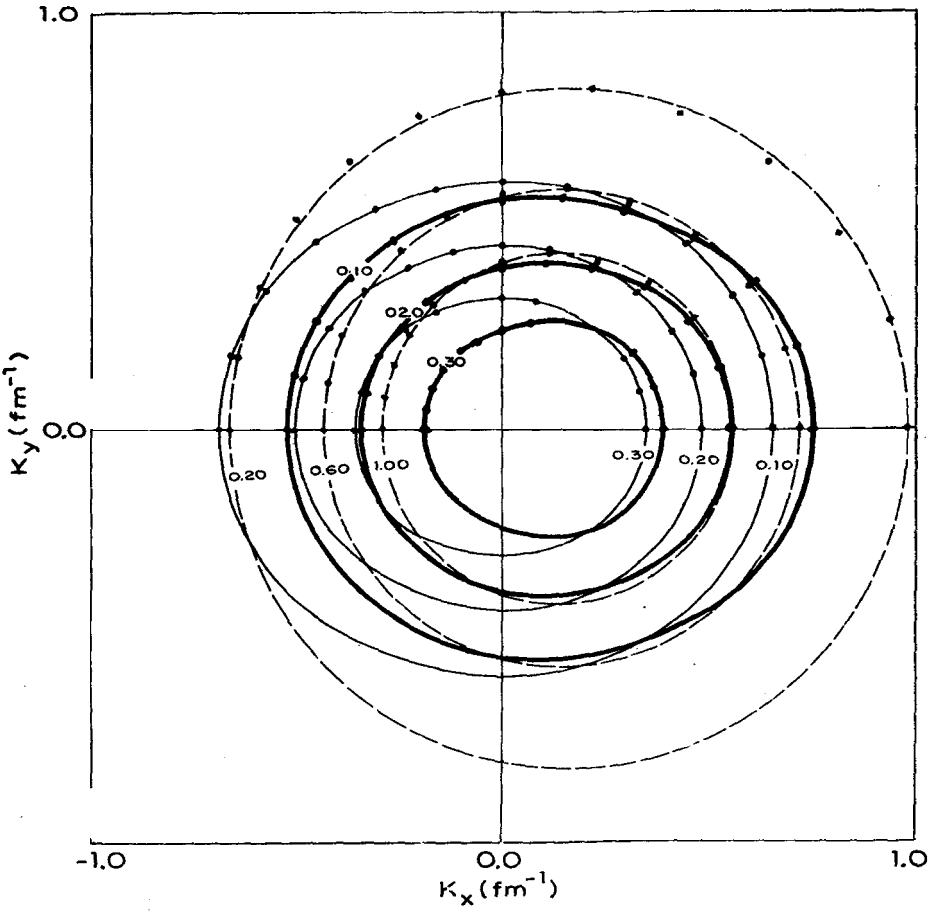

Fig. 2. Contour diagrams of the distorted momentum distributions for the 1*s* state of ^{16}O, at an incident energy of 380 MeV, considering only the real part of the optical potentials (dashed lines), only the imaginary part (thin full lines) and the complete complex potentials (thick full lines). The numbers are the values of the momentum distributions in fm^3.

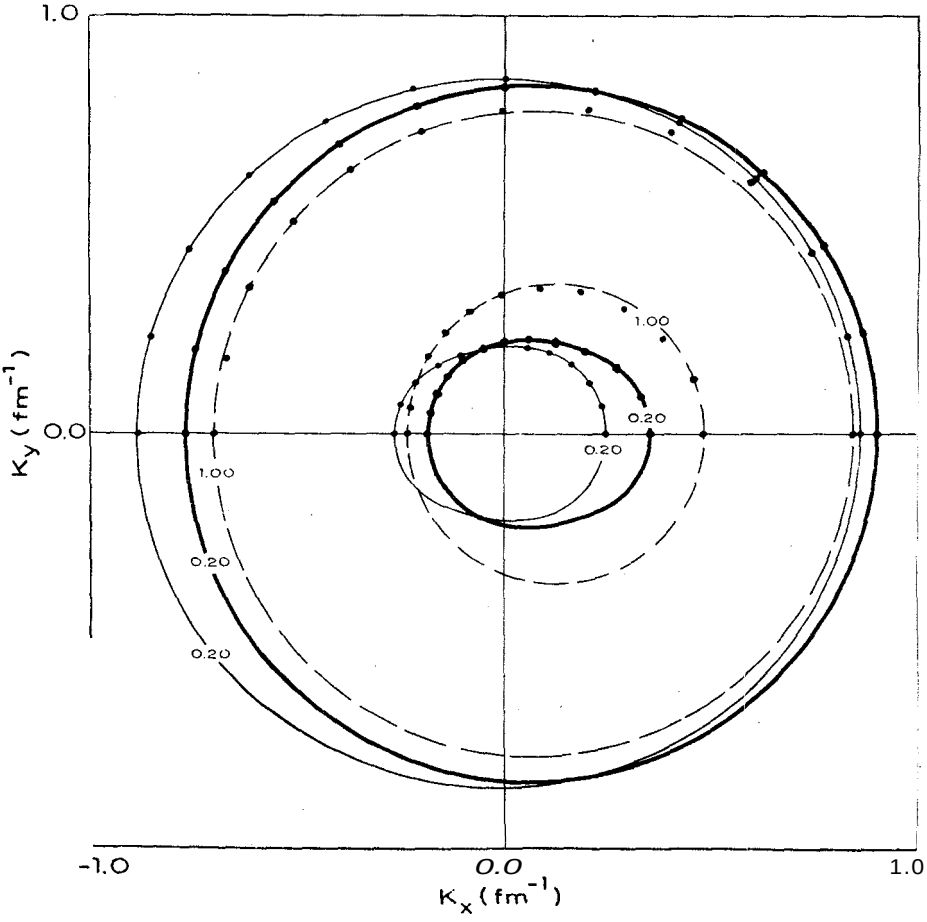

Fig. 3. Same as Fig. 2, for *the* 1*p* state.

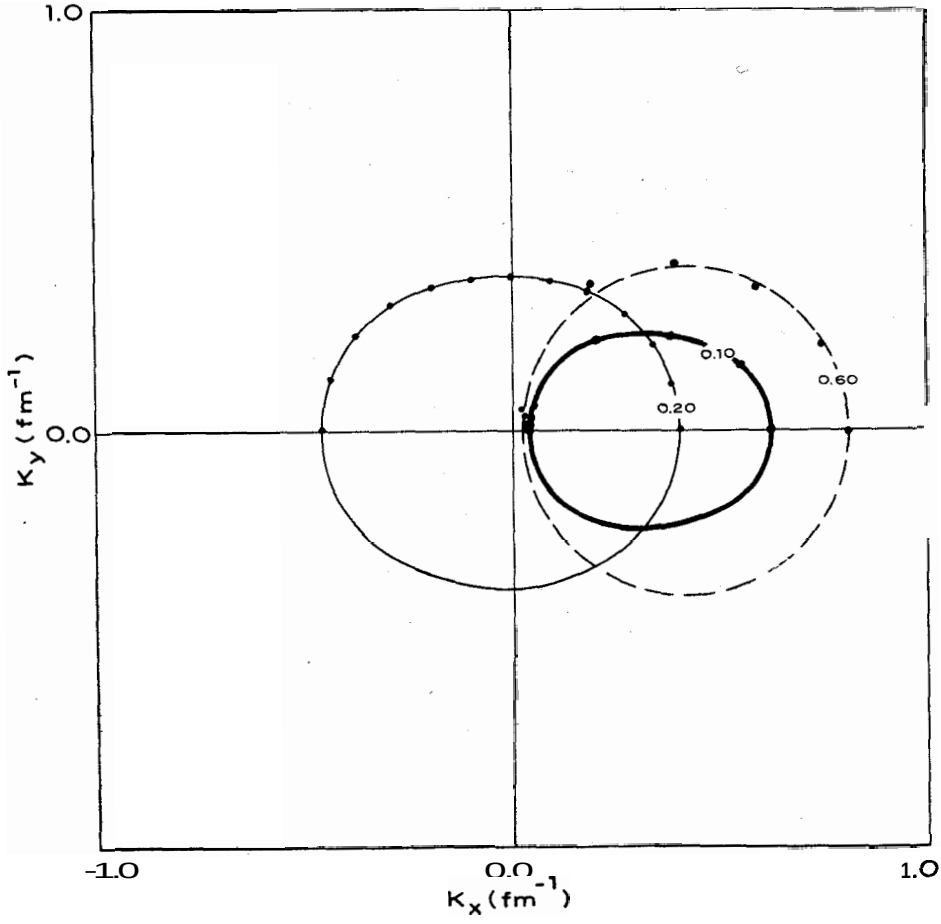

Fig. 4. Same as Fig. 2, for an incident energy of 200 MeV.

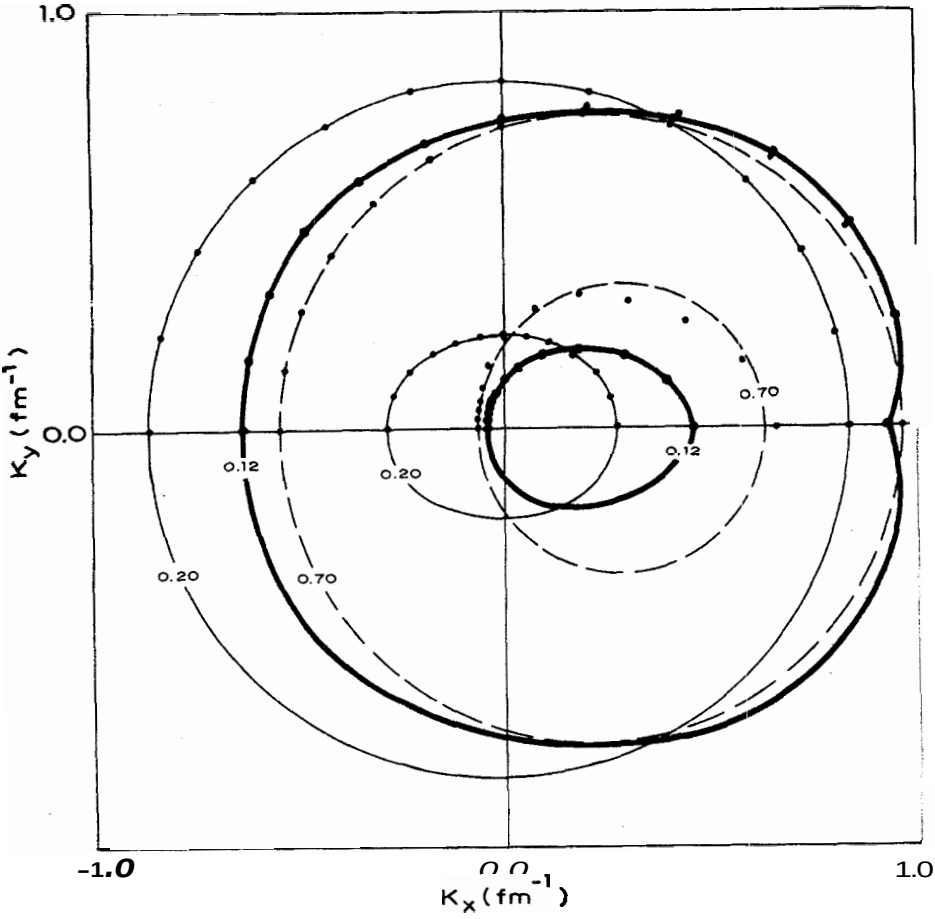

Fig. 5. Same as Fig. 3, for an incident energy of 200 MeV.

3. DISCUSSION AND CONCLUSIONS

As the average optical potential has been taken as a square well, the ef'fective momentum will be constant inside the well and the results are somehow oversimplified; however, this will make the discussion of the effects rather systernatic. General conclusions, of course, would ask for varying the shapes of the potential.

The influence of the real and of the imaginary parts of the optical potentials will be analysed separately. The diagrams where the imaginary parts of the optical potentials have not been taken into account are very approximately circles, with the centres shifted. Dashed lines in Figs. 2-5 represent such circles. As the real part of the optical potential increases with decreasing energy, the shift at 380 MeV is smaller than the one at 200 MeV. On the other hand, the shifts at one incident energy for the lp and ls states are practically the same at 380 MeV. It should be noted that, at 200 MeV, the geometry varies already significantly and thus the variation of the distortion with $\vec{k}$ influences the results strongly.

The shift of the centre of the contour diagram can be compared with the vector addition of the momentum variations of the three protons caused by the real parts of the optical potentials. For the ls state at 380 MeV. such a comparison is very favourable: the shift rneasured on the diagram is 0.14 fm^{-1} whereas the vector addition gives 0.13 fm^{-1}. For the ls state at 200 MeV these results are much less favourable, mainly for the reasons already stated; the figures are, respectively, 0.43 fm^{-1} and 0.27 fm^{-1}. For the lp state an additional problem occurs: as the distorted momentum distribution curves are very steep, it is difficult to construct reliable contour diagrams, due to the large variation of $|g'|^2$ over small ranges of the momenta. Therefore, even for one energy the shifts of the two contour diagrams turn out to be different (in one case, up to a factor of two). An average of the two values obtained for the shifts seems to be a better choice.

The diagrarns where the real parts of the optical potentials have not been taken into account (full thin 1ines in Figs. 2-5) show the two

expected effects: the main effect is, of course, a reduction of the values of $|g'|^2$ and, besides, a deviation from the rotationally symmetric form is observed. These diagrams are "centred" at the origin, but the form is not circular anymore, mainly as a consequence of the effect of the imaginary part of the optical potential. The deviation from the circular form is about the same for all these diagrams, due to the relatively small variation of the imaginary part of the optical potential with energy (Table 2). For the same reason, the value of the momentum for which equal values of $|g'|^2$ occur is ahout the same at the two energies for diagrams with the same angular momentum.

The contour diagrams calculated with the complete complex optical potentials, which could be compared with experimental results, are given by the thick lines in Figs. 2-5. One observes that these diagrams are very close to the ones with a purely imaginary potential, shifted by an amount approximately equal to the one in the diagrams with a purely real potential. This means that the effects of the real and imaginary parts are to a large extent independent of each other. The real part of a more realistic potential would not lead to a constant effective momentum and deviations from the mentioned additive effect would show up.

Incident kinetic energy (MeV)	Nuclear state	$-W_0$ (MeV)	$-W_{1,2}$ (MeV)	$-U_0$ (MeV)	$-U_{1,2}$ (MeV)
380	$1s$	15.4	12.9	3.9	13.3
	$1p$	15.4	13.0	3.9	12.2
200	$1s$	13.1	9.6	10.5	22.4
	$1p$	13.1	10.2	10.5	20.8

Table 2. Values of the square well optical potentials $V_i = U_i + iW_j$ $(j = 0,1,2)$. Index 0 refers to the incident proton. Indices 1,2 refer to the outgoing protons $(V_1 = V)$.

The simple calculations presented in this note do not allow to draw more quantitative conclusions on the contour diagrams. The square well distorting potential is rather unrealistic and for actual comparison with experiments better optical potentials should be used. For more realistic potentials, the real partwill in general also modify the form of the diagram, which will deviate more strongly from the circular form; the effect of the imaginary part on the tail of the wavefunction may also influence appreciably the results, since a more realistic absorption will give the proper weight to the nuclear surface.

Actually, the main purpose of the present work has been to understand semiquantitatively the usefulness of the contour diagrams. Nevertheless, from the results obtained, it seems to be clear that measurements leading to such contour diagrams would be welcome, because if compared to more realistic calculations a better picture of distortion could be obtained.

One final remark is in place. Because of the shift of the centre of the contour diagrams caused by the real parts of the optical potentials, care must be exerted when in (p,2p) experiments the momentum distribution is scanned in a direction orthogonal to, e.g., the momentum transfer. In this case, due to the additional "momentum" introduced by the real potential, one may be sweeping the momentum distribution in such a way as to miss completely the minimum (≃ zero) of a $1p$ distribution on the maximum of a 1s distribution, thus falsifying the results.

We would like to thank Dr. Th. A. J. Marís for several helpful discussions and suggestions, and C. Schneider for his valuable assistance at various stages of this work.

REFERENCES

1. H. Tyrén, Th.A.J. Maris and P. Hillman, Nuovo Cimento 6 (1957) 1507.
2. Th.A.J. Maris, P. Hillman and H. Tyrén, Nucl. Phys. 7 (1958) 1.

3. V.E. Herscovitz, G. Jacob and Th.A.J. Maris, Nucl. Phys. A *109* (1968) 478.
4. G. Jacob and Th.A.J. Maris, Rev. Mod. Phys. 45 (1973) 6.
5. A. Watt, Phys. Lett. 27 *B* (1968) 190.
6. C. Gustafsson and T. Berggren, Phys. Lett. 35 *B* (1971) 546.
7. P. Schwaller, B. Favier, D.F. Measday, M. Pepin, P.U. Renberg and C. Serre, CERN 72-13 (1972).
8. J. Dabrowski and A. Sobiczewski, Phys. Lett. *5* (1963) 87.